Formulation and in-vitro Evaluation of Ethosomes using Anastrozole as a Modeling Drug

Neven Nasef AlEbadi*, Mohammed Sabar Al-Lami**
***College of Pharmacy, University of Basrah, Basrah, Iraq .**

Article Info:

Received Dec 2022
Accepted Dec 2022
Corresponding Author email:
neven.n.phr@uobasrah.edu.iq
orcid: https://orcid.org/0000-0002-9540-8804

DOI:

Abstract:

A series of nine novel 4, 5-dihydro-1H-pyrazole-1-yl acetate derivatives (IVa-i) by Shahlaa et al. was investigated in vitro for their antiproliferative activity against two cancer cell lines, breast cancer cell line (MCF-7) and lung cancer cell lines (A549), According to

Key words: Pyrazole, anticancer, 4, 5-dihydro-1H- Pyrazole, MCF-7, A549

تصنيع وتقييم الايثوسومات خارج الجسم باستخدام عقار الاناستروزول كنموذج

نيفين نصيف جاسم *، محمد صبار عبد الرضا اللامي*
***جامعة البصرة كلية الصيدلة**

الخلاصة:

أناستروزول (ANZ) هو مثبط قوي للأروماتيز II غير الستيرويدي (AI) يستخدم لتقليل أو تأخير تطور ورم الثدي لدى بعض النساء. نظرًا لأن تناول ANZ عن طريق الفم يرتبط غالبًا بأعراض جانبية جهازية شديدة. لذلك، يمكن اعتبار الإيثوسومات المحملة بـ ANZ لتوصيل الأدوية عبر الجلد بديلا(TDDS) بديلا جيدا.

تهدف هذه الدراسة إلى تكوين جسيمات الايثوسومات المحملة بالاناستروزول وتقييمها مختبريا.

تم استخدام طريقة ترطيب الفيلم لتحضير الايثوسومات المحملة بـ .ANZ باستخدام نسب مختلفة من فوسفاتيديل كولين الصويا والإيثانول بنسب مختلفة ، تم تقييم حجم الدقائق ومقياس التشتت المتعدد PDI باستخدام جهاز قياس تشتت الضوء التفاضلي (DLS) ، وفحص التفاعل بين المكونات باستخدام FTIR، وكذلك تقييم كفاءة حصر الدواء داخل الحويصلات ،وتحرير الدواء منها . كما تمت دراسة تأثير النسب المئوية للمكونات المختلفة ومتغيرات عملية الصوتنة على حجم جزيئات الجسيمات ومقياس التشتت المتعدد.PDI

كان للعينة المفضلة التي تحتوي (20% ايثانول و2% من فوسفاتديل كولين الصويا وتعرضت لموجات صوتنة بقوة 300 واط) قطر جسيم 127.75 ± 0.36 نانومتر و 74.7136 ± 3.457٪ كفاءة حصر داخل الحويصلات ووجد انها تتبع نموذج كوسماير بيباس لتحرير الدواء حيث ، R2 = 0.977 و n=0.737

الكلمات المفتاحية: الايثوسومات , الاناستروزول , إيصال العلاج عبر الجلد , فوسفاتديل كولين الصويا

Introduction

The key benefit of the transdermal drug delivery system is to overcome the difficulties through the oral route. The major advantages of Transdermal Drug Delivery System TDDS are improving bioavailability with controlled drug release, reduced side effects, and avoiding first-pass metabolism. TDDS documented itself as an essential portion of the Novel Drug Delivery System (NDDS) with the prescribed dosage forms. In TDDS, a drug is administered at relatively low amount to the surrounding area by a patch or other system, which circulates transversely through the skin barrier. Throughout the distribution course, the drug enters directly through the skin into the bloodstream;

hence, a higher concentration is obtained in the blood (1).

Ethosomes are transdermal drug delivery carriers consisting of phospholipid, cholesterol, alcohol, water, and propylene glycol with different concentrations. They are soft and flexible carriers, with size ranging from 30 nm to several microns that could penetrate the stratum corneum and enhance the permeation of various drugs (2). Greater flexibility is conferred by the Ethanol's presence in the vesicles compared to normal liposomes; this, together with the permeation-enhancing action of Ethanol itself that is attributed to the ability of Ethanol to fluidize the stratum corneum lipids, results in a higher quantity and deeper penetration of the medication through the skin. (3). Ethosomal vesicles are structurally composed of a phospholipid bilayer and an inner aqueous core containing a drug. Ethanol acts as an efficient penetration enhancer that makes the transportation of medicinal agents into a deeper skin layer and systemic circulation very easy and effective. They can entrap a wide variety of molecules, including hydrophilic, lipophilic, and high molecular weight substances. They can deliver the drug across the skin under occlusive and non-occlusive conditions (4).

Anastrozole (ANZ) is a potent non-steroidal aromatase Type II inhibitor (AI) that can selectively inhibit aromatase, this inhibition leads to lower estrogen levels, decreasing tumor mass or delaying the progression of tumor growth in some women (5). All optimal features needed for drug delivery across skin like dosage of 1 mg/day (low dosage), the solubility of 0.5 mg/ml, partition coefficient of 3.5, a molecular weight of 293.3 Daltons, and a half-life of 46.8h are in ANZ, therefore this drug has been used as a model drug for In vitro characterization of ethosomes (6).

The research was characterized by use of only Ethanol and Phosphatidyl choline in preparation of ethosomes, while the previous studies used cholesterol and/or propylene glycol in addition to Ethanol and Phosphatidyl choline (7-9). The study of the effect ultrasonication pulse ratio on Vesicle size and PDI of ethosomes which is included in this research considered a characteristic study for the research

The aim was formulation of ANZ-loaded ethosomes and characterization of the formulated ethosomes for particle size, PDI, entrapment efficiency and in vitro drug release in addition to P-XRD and FTIR.

Materials and Methods

Materials

ANZ from (Baoji Guokang Bio-Technology Co., Limited, China) and Soy phosphatidyl choline were purchased from Hangzhou Hyper Chemicals Limited China, Franz diffusion cells and Probe sonicator (Biobase-China)

HPLC method for determination of ANZ

A modified USP-validated method was used for ANZ to be detected via HPLC (Knauer-Germany). Where the mobile phase composed of Acetonitrile: Water (60:40) and diluent same as the mobile phase were used, standard solution of 50µg/mL of ANZ powder in diluent used to determine the major peak and retention time.

(Vertex Column C18 Eurosphere-100, 250 x 4mm), flow rate 1mL /min, injection volume 20 µl, uv detector at 265 nm [8]

Preparation of Ethosoms

Ethosomes were produced by the film hydration method, Briefly, the lipid mixture which composed of Soy phosphatidyl choline and ANZ powder was dissolved in 10 mL of Ethanol, which was then removed hot air oven at 40˚C for 24 hours, thus obtaining a thin film of dry lipid on the flask wall. The film was then reconstituted by addition of 10 ml of various percentage of Ethanol: Water mixture with stirring [9]; the probe sonicator (Biobase-China) was utilized for vesicle formation and size reduction for 10

min, with different pulse on/off ratios [10]. Twenty-four formulas were prepared, as in Table (1)

Characterization of Prepared Ethosoms

Particle size and Particle Size Distribution

The size of vesicle and size distribution PDI, of the resulting formulae were determined using Dynamic Light Scattering (DLS) Zetasizer-NanoZS (Malvern, UK) (2).

Variables Affecting Particle size and PDI of ANZ-loaded Ethosomes

The parameters utilized to evaluate the ethosmoes and choose the appropriate formula for further research were the particle diameter and polydispersity index at the minimum level.

Effect of Phospholipid Percentage

Because they will affect the size, entrapment efficiency, stability, and penetration ability of the vesicles, the choice of phospholipid type and concentration for the formulation is crucial for the production of the ethosomal system. As in Table (1), different formulas (F1-F4) containing different Soy phosphatidyl choline percentages (0.5%-3%) were prepared (10).

Effect of Ethanol Concentration

Ethanol is an effective penetration booster. By giving the vesicles distinctive properties in terms of size, stability, entrapment efficiency, and increased skin permeability, it plays a crucial role in ethosomal systems. Formulas that contained different percentages of Ethanol (20%-50%) were prepared and tested for differences in particle size and PDI (F5-F8) (11).

Effect of Ultrasonication Power Amplitude

Different sonication power amplitude (225, 300, 375 Watt) was applied on formulas (F9-F10).

Effect of Ultrasonication Pulse Ratio on/off

Different ultrasonication pulse ratio on/ off has been applied on ethosomal formula to examine its influence on particle size and PDI (F11-F12).

Table (1): Different composition percentage and condition used for preparation ethosomal formulas loaded with 1 mg ANZ

Formula	Soy Phosphatidyl choline %	Ethanol %	Power watt	Pulse ratio on/off (sec)
F1	0.5	40	300	1/3
F2	1	40	300	1/3
F3	2	40	300	1/3
F4	3	40	300	1/3
F5	1	20	300	1/3
F6	1	30	300	1/3
F7	1	40	300	1/3
F8	1	50	300	1/3
F9	1	20	225	1/3
F10	1	20	375	1/3
F11	1	20	300	1/7
F12	1	20	300	1/10

Fourier Transform InfraRed Spectroscopy

The solid powder could be obtained by crushing the membrane sample until finely ground solid powder is obtained. After that, the sample powder needs to be mixed with powdered potassium bromide (KBr) and pressing the mixture under high pressure. The ratio between sample powder and KBr is about 1:100 to form a very homogeneous KBr pellet. The resultant KBr pellet can be inserted into a holder in the FTIR spectrometer to get the FTIR spectrum (12).

X-Ray Diffraction

The sample crystallography was obtained using the random mounts method. In this method, particles were packed to a flat surface onto a sample holder to assume different crystallite orientations and ensure reflections from various planes, the angle for testing was (5-80) degrees (13).

Entrapment Efficiency

The dialysis centrifugation method was used to determine the drug-loaded ethosoms' entrapment efficiency. Briefly, 1mL of ANZ-loaded ethosoms was placed into a dialysis bag (molecular weight cutoff [MWCO] 8000–14,000 Da) and two ends of the dialysis bag were tied. This dialysis bag was then placed into a centrifuge tube and centrifuged for two hours at 6000 rpm at 25° C, the filtrate from dialysis bag has been collected and by the use of HPLC the ANZ content in the filtrate has been estimated which represent the free ANZ within formula (Wf). The total drug contained in the ANZ-loaded ethosoms was determined by disrupting the mixture with Methanol. It is done by diluting the formula trace in the dialysis bag with enough Methanol to disrupt the vesicle and again using HPLC the ANZ content within vesicle has been dete cted, the total drug contained within formula was the summation of free ANZ and ANZ entrapped within vesicle. (14)

The following equation was used to compute the entrapment efficiency:

EE %= (wt – wf / wt) ×100%. ------eq 1

Where wt is the total drug amount in the formula

Wf is the amount of free drug in the formula

The *In-vitro* Release Studies

The precise volume, which comprised 1 mg of ANZ in the selected formulae was placed into dialysis membrane (2,000-8000MWT cut-off). The same was done to the hydroethanolic solution of the medicine as control. The fastened two ends membrane was placed in a beaker with 100 mL of pH 7.4 phosphate buffer and stirred at a speed of 60 rpm while the temperature was 37 °C.1mL of the medium was removed at distinct time intervals. To maintain a continuous sink condition, a 1 mL of new phosphate buffer pH 7.4 was replenished simultaneously. The concentration of the medication released from a tested sample was determined using HPLC (15)

Release Kinetics Modelling

To study the release kinetics, data obtained from *in-vitro* drug release study for ethosoms was fitted to the following kinetic models: zero order (cumulative drug amount released vs. time), first order (log of the cumulative drug percentage remaining vs. time), Higuchi's model (cumulative drug percentage released vs. square root of time) and Korsmeyer-Peppas (log of the cumulative drug percentage released vs. log time) as in equations 2-1, 2-2, 2- 3and 2-4 respectively, to find the best-fitted line for predicting the drug release mechanism (16)

Zero order :	$\mathbf{Qt = Q_0 + K_0 t}$	..…Eq (2-1)
First order:	$\mathbf{Log\ Q_t = Log\ Q_0 - k_1 t / 2.303}$	…..Eq (2-2)
Higuchi :	$\mathbf{Q_t = K_H\ t^{1/2}}$	…..Eq (2-3)

Korsmeyer-Peppas: $\mathbf{Q_t / Q_0 = K_P t^n}$ …. Eq (2-4)

Where: Qt is the drug amount released at time t, and Q_0 is the initial drug amount in the ethosomes. k_0, k_1, k_H, and k_P are the release rate constants of zero order, first order, Higuchi and Korsmeyer–Peppas respectively. While n is the release exponent indicating the release mechanism from spherical matrices. When n < 0.43, a Fickian diffusion drug release mechanism occurs, while if 0.43 < n < 0.85 a non-Fickian or anomalous diffusion is predominant. The Higuchi model (Eq.2-3) is related to a special case of Korsmeyer-Peppas (Eq.2-4) where n=0.5 (17).

Statistical Analysis

To evaluate the difference between the results of studied formulations, the one-way analysis of variance (ANOVA) test using Microsoft Excel Add ins 2019. The significance level was specified at α = 0.05, and the difference between data with (P <0.05) was considered statistically significant while if the difference was (P>0.05) then it will be considered as non-significant, All the results were illustrated as the mean values ±standard deviation (SD) in three replicates (n=3).

Results and Discussion

Drug detection by HPLC

The drug retention peak appeared at a time of 4.65 minutes of drug standard sample (20 µL) passage across a column with a peak width of 0.17 and intensity of 96 %,

Characterization of prepared ANZ-loaded ethosoms

Characterization of particle size and PDI

Variables Affecting Particle size and PDI of Ethosomes

Vesicle size is crucial for topical drug delivery systems since smaller vesicles transmit their contents more effectively across skin deeper layers (18). The index of polydispersity (PDI). The term “polydispersity” (or “dispersity”) is used to describe the level of non-uniformity of the particles size distribution. Also referred as heterogeneity index.

This index is scaled and non-dimensional, so values bellow 0.05 are typically observed with very monodisperse standards. A sample having PDI value above 0.7 is considered to have broad particle size distribution and a is usually not acceptable for dynamic light scattering DLS analysis. When dealing with data that lies between these two extreme values of PDI, (i.e., 0.05–0.7) various size distribution strategies are used (19).

Table 2 shows the particle size and PDI of the prepared formulas.

Table (2): The particle size and PDI ethosomal formulas (Average ±SD n=3)

Formula	Average particle diameter nm	PDI
F1	372.75±1.823	0.408±0.008
F2	234.85±2.28959	0.433±0.0045
F3	528.7±2.092845	0.177±0.0185
F4	818.2±1.496663	0.368±0.0005
F5	127.75±0.355903	0.261±0.009
F6	156.6±1.5	0.359±0.026
F7	379.85±0.55	0.369±0.0195
F8	416.25±1.15181	0.354±0.015
F9	146.75±0.873053	0.347±0.0065
F10	412.1±1.070825	0.456±0.0065
F11	616.15±1.144067	0.39±0.0025
F12	187.05±1.033871	0.253±0.059

Effect of Phospholipid Percentage

As (Figure 1 A and B) shows while the PDI declined with higher Soy phosphatidyl choline percentage, the rise in Soy phosphatidyl choline percentage results in a significant ($p \leq 0.05$) increase in particle size. This could be because as Soy phosphatidyl choline content raised, more Soy phosphatidyl choline molecules may have been available to serve as surfactants which stabilize and facilitate the production of more uniform vesicles (20).

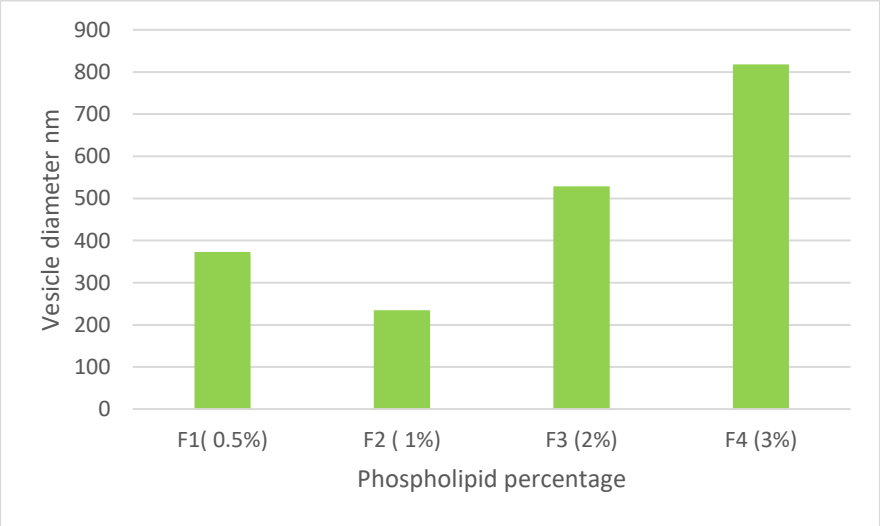

Figure (1) A: The effect of phospholipid concentration on particle diameter

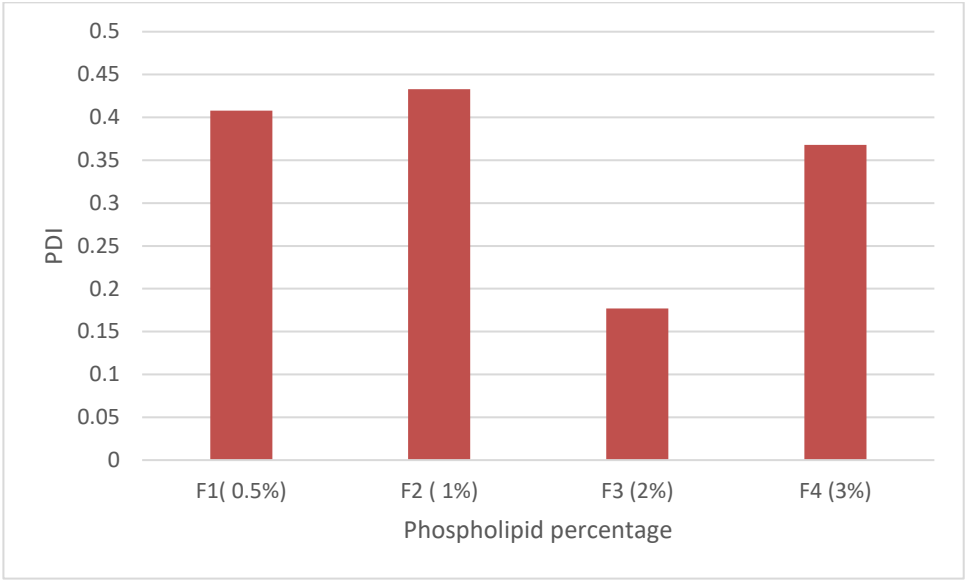

Figure (1) B: The effect of phospholipid concentration on PDI

Effect of Ethanol Concentration

Although Ethanol can increase the membrane fluidity of ethosoms and improve their stability, it has been demonstrated that Ethanol concentrations greater than 45% (*w/w*) reduce the value of entrapment efficiency. Perhaps because higher Ethanol contents may cause the membrane to leak, thus Ethanol concentrations in ethosoms should be kept within a certain range (21). The impact of Ethanol concentration on the particle diameter and PDI was studied in F5-F8 (Figure 2 A and B). A rise in Ethanol percentage above 30% increases particle size significantly ($p \leq 0.05$) but had little effect on PDI. This phenomena may be brought on by the high concentration of Ethanol, which may cause the lipid vesicles to be disrupted or solubilized and hence increasing vesicle size (3).

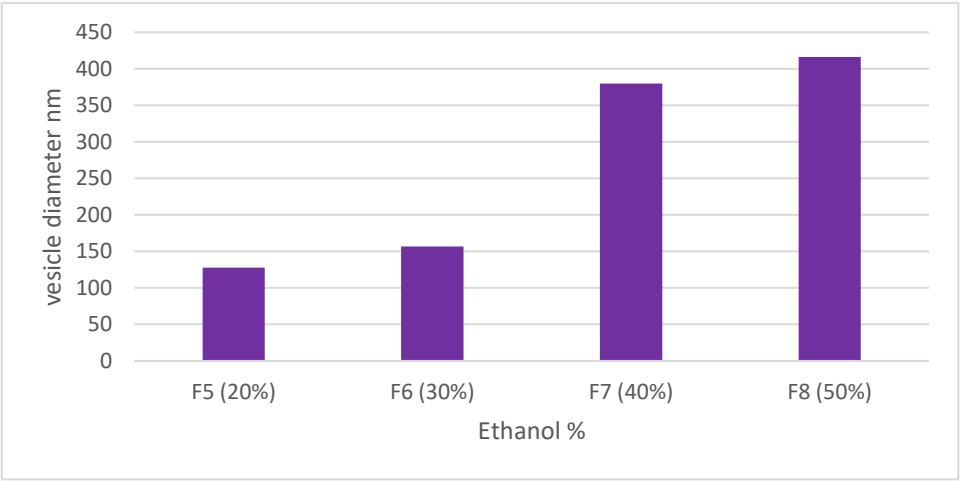

Figure (2) A: The effect of Ethanol concentration on the particle diameter of the prepared ethosmal formula

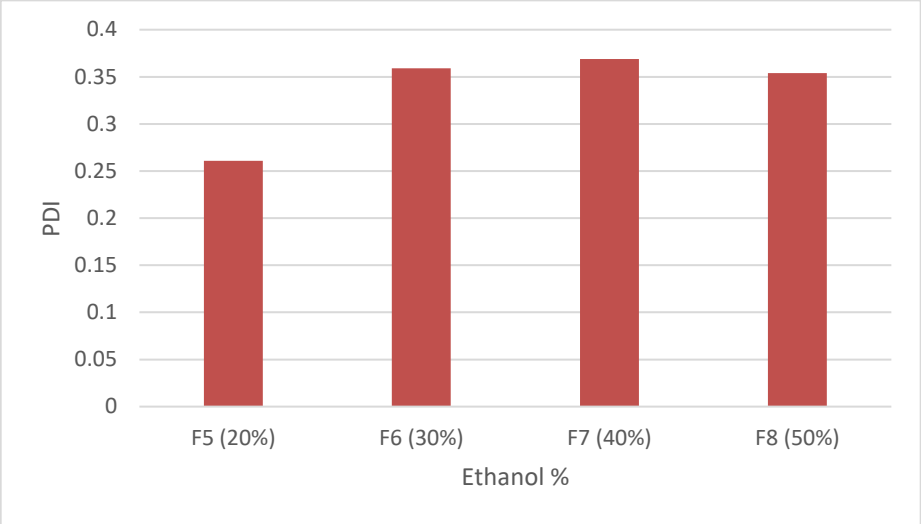

Figure (2) B: The effect of Ethanol concentration on the PDI of the prepared ethosmal formula

Effect of Ultrasonication Power Amplitude

Ultrasonication is a widely used high-energy method to reduce the droplet size of nano preparation. In this method, mechanical vibrations from ultrasound waves (> 20 kHz) create sinusoidal pressure variation in the system. This processing leads to microjet and shock-wave impacts and collisions between particles, resulting in particle-size reduction. Even though it is crucial to comprehend that the particle size once it reaches equilibrium during the ultrasonication process, it is vital to know the dynamic pathways to reduce the processing time and use optimum power, thus avoiding the over-supply of energy, which may result in larger particle size than expected (22)

Sonication is a widely used technique for encapsulating nanoparticles. Large multilamellar vesicles (MLVs) can be prepared by hydrating dry phospholipid films and subjecting them to vigorous mixing. Sonication power can break up these vesicles into smaller, unilamellar vesicles (ULVs) of known size, which are more popular for encapsulation. Inadequate sonication will prevent MLVs from reducing to their ideal size, while excessive sonication will harm the vesicles by creating free radicals and causing aggregation (23). The sonication power affects the particle size and PDI of F5, F9, F10 (Figure 3 A and B). The changed sonication power showed a significant ($p \leq 0.05$) impact on particle size, with the best result obtained with the power of 60 % (300watt).

When increasing ultrasonication power to 75%, the mean particle size showed a slight increase. This result might be justified by the possibility that, when the vibration amplitude increased, bubbles may grow so large that the time available in the adjacent rarefaction cycle will not be sufficient for them to collapse hence reducing cluster (24).

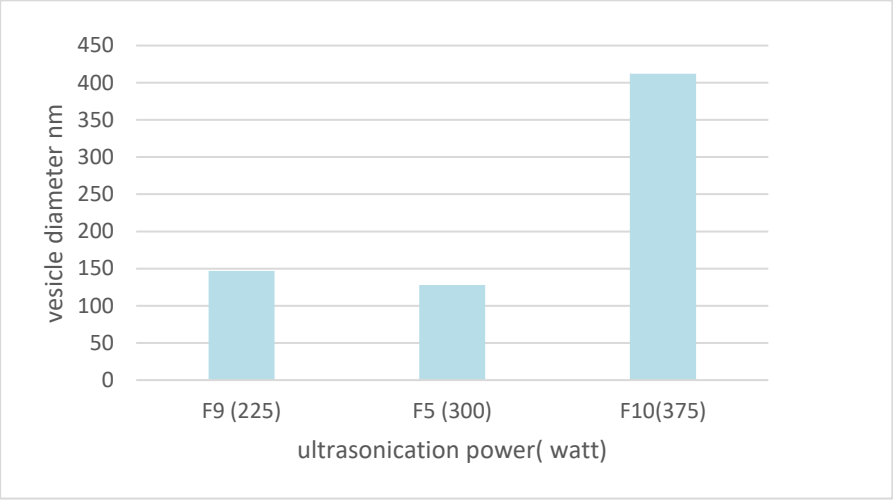

Figure (3)A: The effect of ultrasonication power on particle diameter of the prepared ethosmal formula

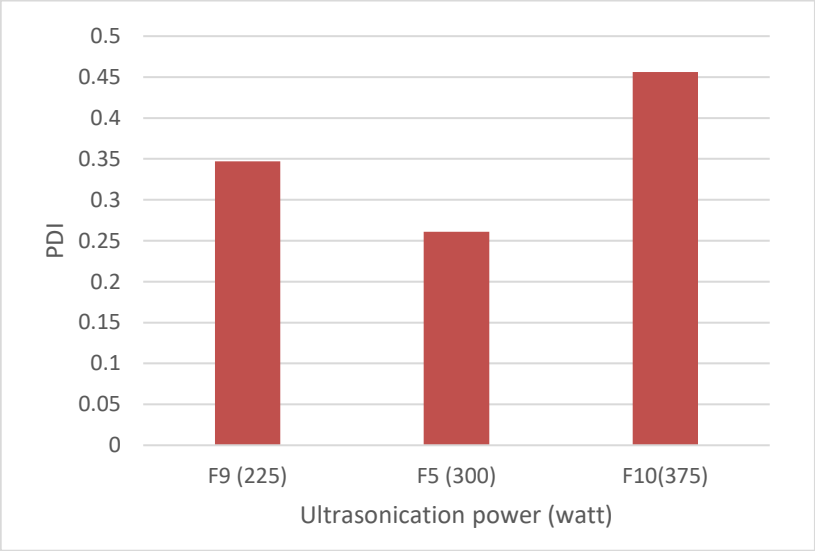

Figure (3)B: The effect of ultrasonication power on PDI of the prepared ethosmal formula

Effect of Ultrasonication Pulse Ratio on/off

The ultrasonication pulse ratio might be adjusted to keep the temperature of the formula at around 35 degrees Celsius. (24). The effect of pulse ratio changes on particle size and PDI in F5, F11, F12 was studied (Figure 4 A and B), Higher pulse ratio increases energy transfer to the medium, which increases medium temperature Sonication efficiency, however, increases when the medium temperature is low. When the temperature of the medium increases due to cavitation, the medium expands, leading to the production of less energetic shock waves from bubble implosion and hence less size reduction (25). The results showed the significant ($p \leq 0.05$) effect of pulse ratio on particle size and PDI.

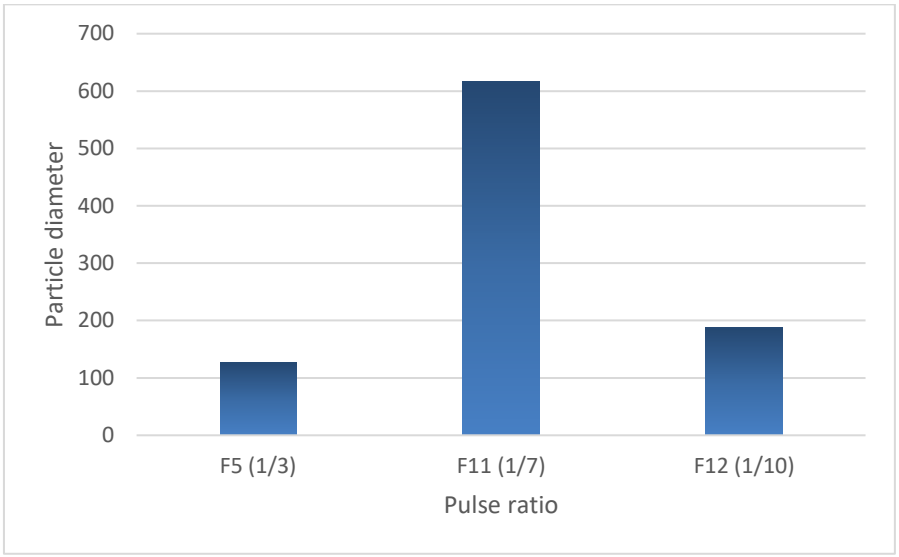

Figure (4)A: The effect of ultrasonication pulse ratio on particle diameter of the prepared ethosmal formula

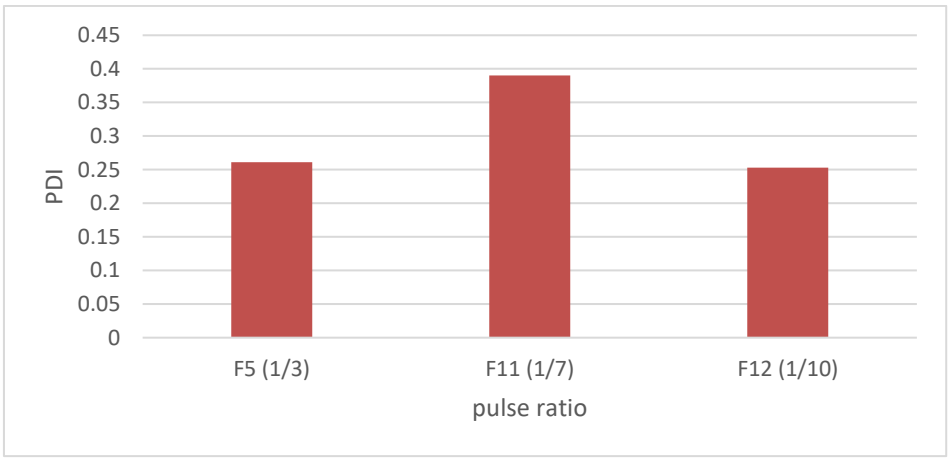

Figure (4)B: The effect of ultrasonication pulse ratio on PDI of the prepared ethosmal formula

FTIR

FTIR study was done for F5 (which composed of 20% Ethanol ,1% Soy phosphatidyl choline and subjected to 300-Watt ultrasonication power with 1/3 pulse ratio) because it shows the best particle size and PDI.

Figure (5-a) for pure ANZ showed characteristic peaks at: 3101.94–2981.41cm–1 aromatic C–H stretch of benzene, 2361.41-2235.09 cm–1 representing aliphatic C≡N stretch of nitrile, and 1604.48–1501.31 cm–1 representing C=N hetero aromatic stretching, 1357.64-1200.47 representing CH3 bending (26). Figure (5-b) for Soy phosphatidylcholine showed the prominent absorption bands at 3163.65 for =C-H stretching, at 2915.84 cm−1 (for C H stretching vibration of methylene group), 1736.58 cm−1 (for C =O stretching vibration) 1610 cm-1 (for C=C stretching) ,1081.87 (for PO2- stretching), band around 718 cm−1 for CH2 rocking (27). Figures (5-c and 5-d) show The FTIR peaks of the physical mixture and selected formulation(F5) respectively exhibited no drug or Soy phosphatidyl choline band change in strength or position, indicating

there was no drug/ Soy phosphatidyl choline interaction (9).

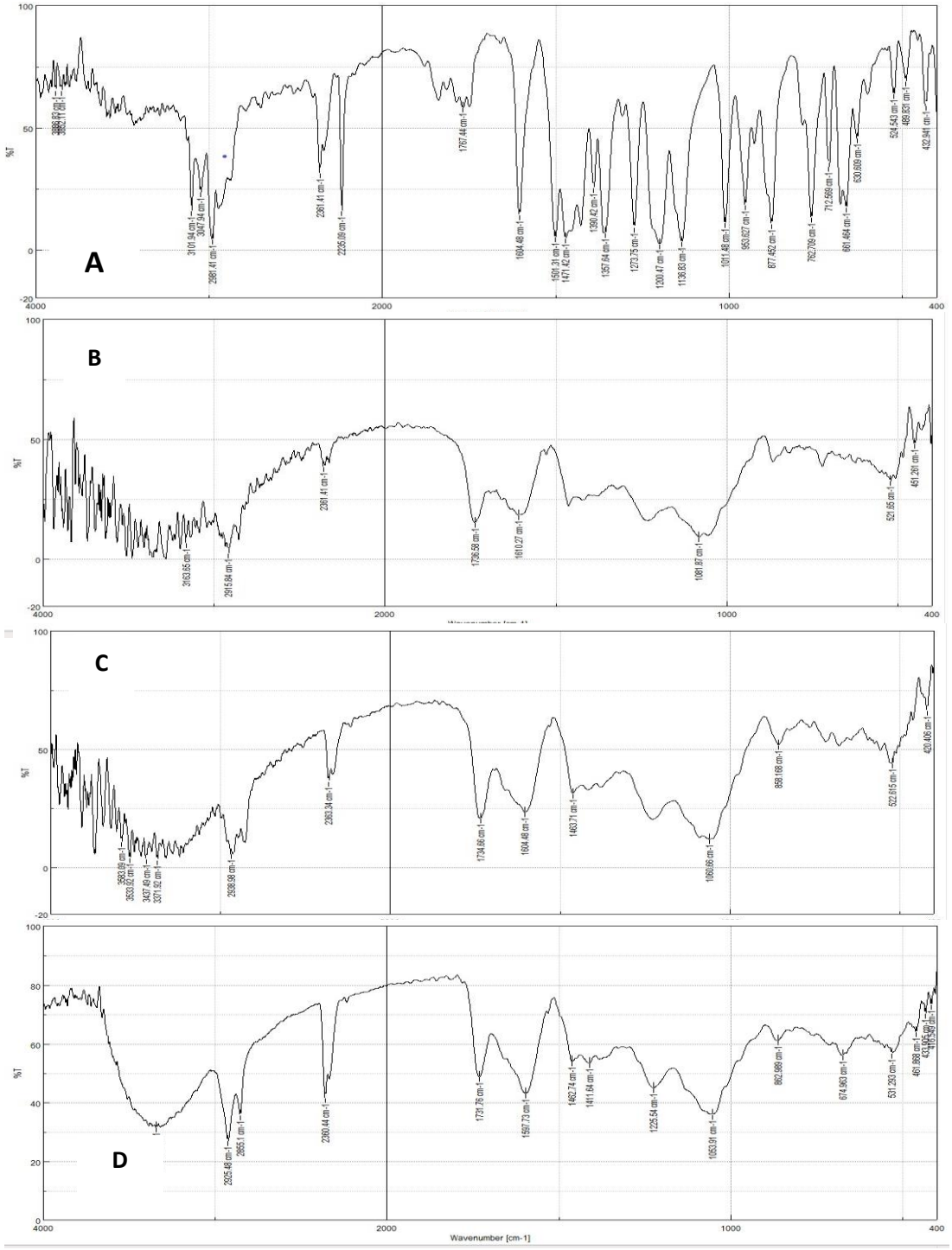

Figure (5) FTIR spectra of A: ANZ, B: Soy phosphatidyl choline, C: physical mixture, D: F5

Powder X-ray diffraction

Figure (6) represent the P-XRD for pure ANZ, it showed the sharpest diffraction peak at 18.5863, while the Soy phosphatidyl choline showed a characteristic diffraction broad peak at 19.8798; the ANZ diffraction peak was also present in the curve of the physical mixture, which proved that the crystal form of ANZ was the same with that of the pure drug powder. In contrast, the characteristic diffraction peak of ANZ

disappeared in the curve of ethosoms powder (F5), indicating a disordered crystalline state of ANZ in ethosome. These results proved that ANZ had been successfully incorporated into the lipid matrix of ethosoms in an amorphous or disordered state (28).

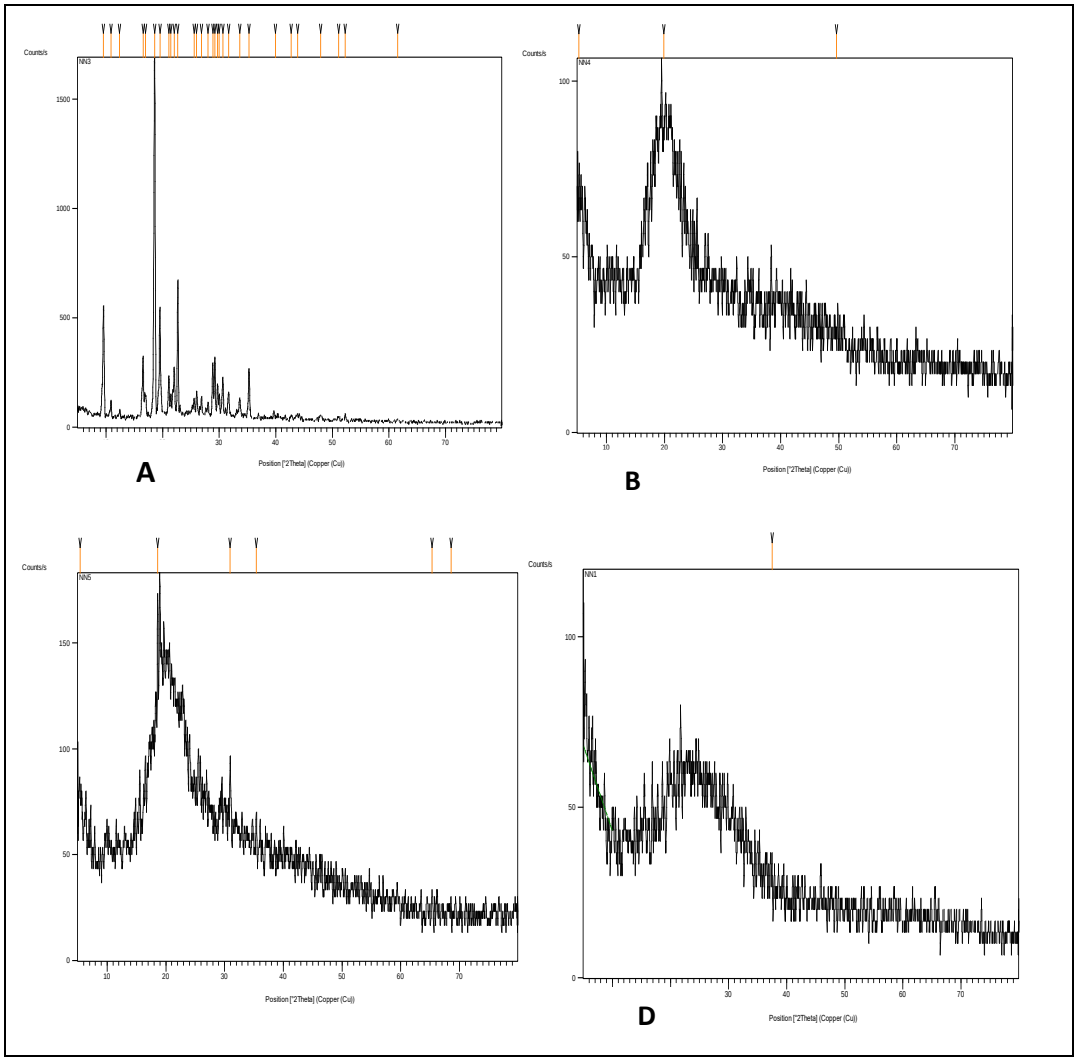

Figure (6): X-Ray Diffraction chromatogram for A: pure ANZ, B: Soy phosphatidyl choline, C: physical mixture, D: F5

Entrapment efficiency

Depending on the results from particle size and PDI characterization (F5, F6 and F7) which have the best particle size and PDI was chosen for further characterization. Table 3 shows the entrapment efficiency of ethosoms and drug contained within the formulas F5, F6 and F7. The relatively high entrapment of ANZ within the ethosomal vesicles is explained by multi-lamerality and the presence of Ethanol content (29). There was increase in the entrapped amount of drug was observed with an increase in Ethanol concentration, but when Ethanol concentration exceeded 30%, a decline in percent drug entrapment was observed. Improvement in aqueous solubility of ANZ was achieved with higher concentration of Ethanol, which could result from its co-solvent effect. Therefore, the more drug amount could be accommodated in the aqueous core of the vesicles however, drug leaked from the fluidized bilayer of the vesicle as the

Ethanol concentration rose above 30% as a result of Ethanol's fluidizing effect on lipid, which causes the lipid bilayer to leak (30).

Additionally, the effectiveness of entrapment rises as lecithin concentration rises up to a certain limit (i.e 3%) above which drug permeability is reduced (18).

Table (3): The EE % and drug content of selected ethosomal formulas

Formula	F5	F6	F7
EE%	74.7136 ± 3.457	75.6453 ± 2.541	68.7112 ± 2.411
Free drug %	22.00203 ± 0.5981	20.879 ± 0.764	27.887 ± 1.203
drug content %	96.7156 ±1.243	96.5243 ±0.853	96.5982 ± 1.006

In-vitro ANZ Release Study

According to DLS, and entrapment efficiency results, F5 (which composed of 20% ethanol and 1% soy phosphatidyl choline and subjected to 300-Watt ultrasonication power with 1/3 sec ultrasonication pulse ratio on /off) shows the best particle size and PDI was chosen to be tested for the in-vitro drug release. In the case of hydroalcoholic drug solution, (99.8724 ± 1.089966) of the drug was released during 2-3 hours, whereas the maximum drug amount released from ethosomes takes 5-6 hours, demonstrating that the drug diffusion from ethosomal bilayers is the rate-limiting step in overall drug permeation through the cellophane membrane (31). There was no significant ($p>0.05$) difference in drug amount released between F5 and control.

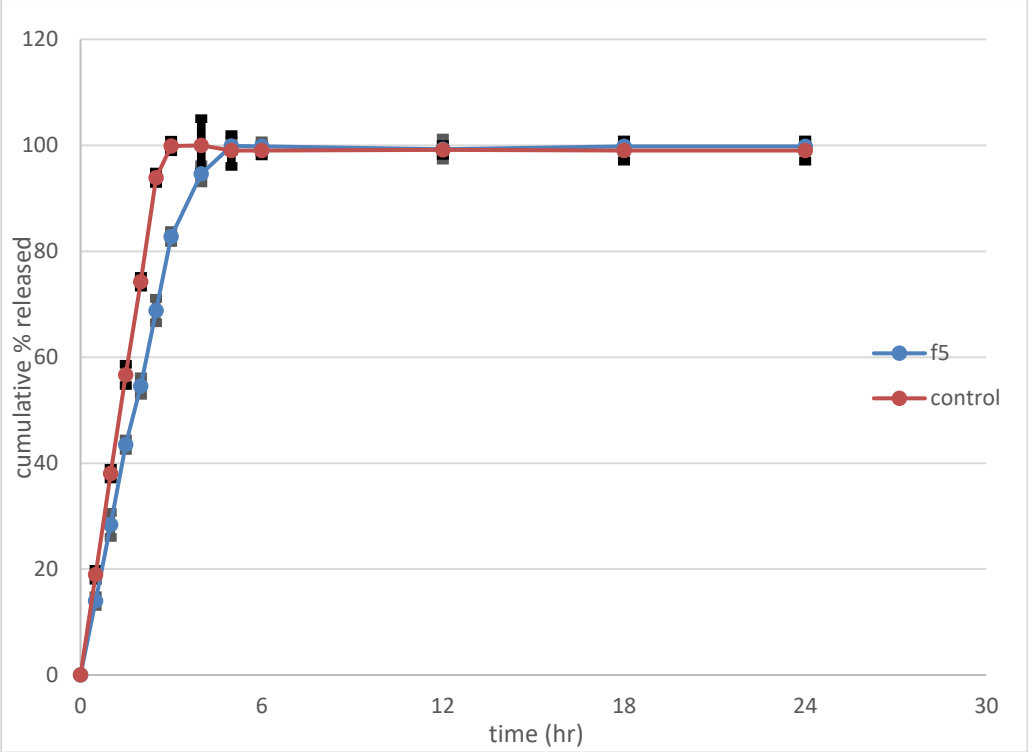

Figure (7): The release profile of F5 and control

Modeling of Ethosomes Release Kinetic

The selected formulas of ANZ-loaded ethosomes in-vitro release profile were fitted on various kinetic models; namely, first order, zero order, Higuchi square root of time, and Korsmeyer-Peppas models to calculate the rate constants (k0, k1, KH, kp, and n) and the regression coefficient (R2), the obtained fitting parameters are demonstrated in the Table (5).

In the Korsmeyer-Peppas model, fitting only the portion of the cumulative drug release curve below 60% was applied as described previously in literature to determine the (n) value. (17) The obtained data best fits the Korsmeyer-Peppas model with a higher regression coefficient (R2) of (0.9779), indicating that diffusion, matrix erosion, or relaxation contributes to the release mechanism. The formulation showing Korsmeyer (n) values greater than 0.43 (i.e., $0.43 < n < 0.85$) indicates that an anomalous transport mechanism of drug release, which is a combination of Fickian diffusion combined with the non-Fickian mechanisms of matrix erosion and relaxation. (32) A comparison between the obtained release profile of formula F5 and the theoretical kinetic models of Korsmeyer-Peppas, kinetics is shown in the Figure 8.

Table (5): R^2 and K value for F5 release kinetic modeling

formula	zero order		first order		Higuchi		korsmeyer-peppas		
	R^2	k_0 $molL^{-1}S^{-1}$	R^2	K_1 S^{-1}	R^2	K_H $molL^{-1}S^{-1}$	R^2	K_P $molL^{-1}S^{-1}$	n
F5	0.9292	23.652	0.9545	0.462	0.9242	42.734	0.9779	32.937	0.737

Conclusion

From this work it has been concluded that film hydration method is a simple and productive method for preparation of ethosoms. Ethosom's vesicle size, PDI, and entrapment efficiency is affected by ethanol concentration, soy phosphatidyl choline concentration and ultrasonication power and mode, Ethosoms provide a good drug entrapment, and release when compared hydroalcoholic drug solution.

Acknowledgement: authors are thankful to Ministry of higher education and scientific research / University of Basrah for funding this project.

References

1- Jain S, Tripathi S, Tripathi PK. Invasomes: Potential vesicular systems for transdermal delivery of drug molecules. Journal of Drug Delivery Science and Technology. 2021; 61:102166.

2- Amr Gamal F, Kharshoum RM, Sayed OM, El-Ela FIA, Salem HF. Control of basal cell carcinoma via positively charged ethosomes of Vismodegib: In vitro and in vivo studies. Journal of Drug Delivery Science and Technology. 2020; 56:101556.

3- Sakdiset P, Amnuaikit T, Pichayakorn W, Pinsuwan S. Formulation development of ethosomes containing indomethacin for transdermal delivery. Journal of Drug Delivery Science and Technology. 2019; 52:760-8.

4- Nainwal N, Jawla S, Singh R, Saharan VA. Transdermal applications of ethosomes - a detailed review. Journal of liposome research. 2019;29(2):103-13.

5- Caroline S. Zeind and Michael G. Carvalho. Applied therapeutics the clincal use of drug, eleventh ed. Philadelphia Wolters Kluwer Health; 2018.

6- Vidya KS, Lakshmi PK. Cytotoxic effect of transdermal invasomal anastrozole gel on MCF-7 breast cancer cell line. J Journal of Applied Pharmaceutical Science. 2019.
7- BM, Fahmy UA, Abd-Allah FI. Transdermal glimepiride delivery system based on optimized ethosomal nano-vesicles:Preparation, characterization, in vitro, ex vivo and clinical evaluation. International journal of pharmaceutics. 2016;500(1-2):245-54.
8- Bendas ER, Tadros MI. Enhanced transdermal delivery of salbutamol sulfate via ethosomes. AAPS PharmSciTech. 2007;8(4):213.
9- Dave V, Bhardwaj N, Gupta N, Tak K. Herbal ethosomal gel containing luliconazole for productive relevance in the field of biomedicine. 3 Biotech. 2020;10(3):97.
10- Abdulbaqi IM, Darwis Y, Khan NA, Assi RA, Khan AA. Ethosomal nanocarriers: the impact of constituents and formulation techniques on ethosomal properties, in vivo studies, and clinical trials. International journal of nanomedicine. 2016; 11:2279-304.
11- López-Pinto JM, González-Rodríguez ML, Rabasco AM. Effect of cholesterol and ethanol on dermal delivery from DPPC liposomes. International journal of pharmaceutics. 2005;298(1):1-12.
12- Huda S. Kadhium NKM. Preparation and in Vitro Evaluation of Soya Lecithin Based Nano Transfersomal Dispersion for Loxoprofen Sodium. Al Mustansiriyah Journal of Pharmaceutical Sciences, 2019; Vol.19, No.4.
13- Bunaciu AA, Udriştioiu Eg, Aboul-Enein HY. X-Ray Diffraction: Instrumentation and Applications. Critical Reviews in Analytical Chemistry. 2015;45(4):289-99.
14- Niu XQ, Zhang DP, Bian Q, Feng XF, Li H, Rao YF, et al. Mechanism investigation of ethosomes transdermal permeation. International journal of pharmaceutics: X. 2019; 1:100027.
15- Esraa Ghazy AA, Jafar Jaber Al-Tamimi and Nawal Ayash. AJPS, 2016, Vol. 16, No.2Date of acceptance:22-12-20151Nebivolol Hydrochloride Loaded Nanostructured Lipid Carriers as Transdermal Delivery System: Part 1: Preparation,Characterization and In Vitro Evaluation. AlMustansiryah journal of pharmaceutical sciences 2016; Vol. 16 No. 2 (2016): volume 16, Issue 2. 2016.
16- JABBAR ASAJSRP. In-vitro; ex-vivo assessment of anti-inflammatory Tapentadol loaded non-ionic surfactant vesicular systems for effective transdermal delivery. J Sys Rev Pharm. 2020;11(12):636-43.
17- Paarakh MP, Jose PA, Setty C, Christoper G. Release kinetics–concepts and applications. Int J Pharm Res Technol. 2018;8(1):12-20.
18- Paliwal S, Tilak A, Sharma J, Dave V, Sharma S, Yadav R, et al. Flurbiprofen loaded ethosomes-transdermal delivery of anti-inflammatory effect in rat model. J Lipids in health. 2019;18(1):1-15.
19- Danaei M, Dehghankhold M, Ataei S, Hasanzadeh Davarani F, Javanmard R, Dokhani A, et al. Impact of Particle Size and Polydispersity Index on the Clinical Applications of Lipidic Nanocarrier Systems. Pharmaceutics 2018, 10, 57; doi:103390 /pharmaceutics10020057. 2018;10(2):57.
20- Zhao L, Temelli F, Curtis JM, Chen L. Preparation of liposomes using supercritical carbon dioxide technology: Effects of phospholipids and sterols. Food Research International. 2015; 77:63-72.
21- Zhu X, Li F, Peng X, Zeng KJA, Analgesia. Formulation and evaluation of lidocaine base

ethosomes for transdermal delivery. International Anesthesia Research Society DOI: 101213/ ANE0b013e3182937b74. 2013;117(2):352-7.
22- Pratap-Singh A, Guo Y, Lara Ochoa S, Fathordoobady F, Singh A. Optimal ultrasonication process time remains constant for a specific nanoemulsion size reduction system. Scientific Reports. 2021;11(1):9241.
23- Alipour E, Halverson D, McWhirter S, Walker GC. Phospholipid Bilayers: Stability and Encapsulation of Nanoparticles. The Annual Review ofPhysical Chemistry. 2017;68 (1):261-83.
24- Nguyen VS, Rouxel D, Hadji R, Vincent B, Fort Y. Effect of ultrasonication and dispersion stability on the cluster size of alumina nanoscale particles in aqueous solutions. Ultrasonics Sonochemistry. 2011;18(1):382-8.
25- Siddiqui A, Alayoubi A, El-Malah Y, Nazzal S. Modeling the effect of sonication parameters on size and dispersion temperature of solid lipid nanoparticles (SLNs) by response surface methodology (RSM). Pharmaceutical Development and Technology. 2014;19(3):342-6.
26- Hashim AA-J, Rajab NAJIJoPS. Anastrozole Loaded Nanostructured Lipid Carriers: Preparation and Evaluation. J Iraqi Journal of Pharmaceutical Sciences. 2021 ;30(2):185-95.
27- Stuart BH. Infrared spectroscopy: fundamentals and applications: John Wiley & Sons; 2004.
28- Zhai Y, Xu R, Wang Y, Liu J, Wang Z, Zhai G. Ethosomes for skin delivery of ropivacaine: preparation, characterization and ex vivo penetration properties. Journal of liposome research. 2015;25(4):316-24.
29- Iizhar SA, Syed IA, Satar R, Ansari SA. In vitro assessment of pharmaceutical potential of ethosomes entrapped with terbinafine hydrochloride. Journal of Advanced Research. 2016;7(3):453-61.
30- Barupal AK, Gupta V, Ramteke S. Preparation and Characterization of Ethosomes for Topical delivery of Aceclofenac. Indian journal of pharmaceutical sciences. 2010 ;72(5):582-6.
31- Chourasia MK, Kang L, Chan SY. Nanosized ethosomes bearing ketoprofen for improved transdermal delivery. Results in Pharma Sciences. 2011;1(1):60-7.
32- Abed HN. Dabigatran Etexilate Loaded Nanostructured Lipid Carriers: Formulation, Evaluation and Ex-vivo Intestinal Permeation university of baghdad; 2019.